Available online at www.sciencedirect.com
SCIENCE DIRECT
Polymer 47 (2006) 5880–5887
polymer
www.elsevier.com/locate/polymer

Rigid particle toughening of aliphatic polyketone

W.C.J. Zuiderduin[1], J. Huétink, R.J. Gaymans*

Department of Science and Technology, University of Twente, P.O. Box 217, 7500 AE Enschede, The Netherlands

Received 20 March 2006; received in revised form 25 April 2006; accepted 12 May 2006
Available online 5 July 2006

Abstract

The influence of precipitated calcium carbonate particles on the toughening behaviour of aliphatic polyketone has been studied. The calcium carbonate particles had a particle size of 0.7 μm and a stearic acid coating (1%). Composites of 0–31.5 vol% $CaCO_3$ content have been compounded and injection moulded. Studied are the morphology of the composites, the modulus, yield strength, the notch Izod impact strength and the temperature development in the deformation zone by infrared thermography.

The thermal properties of the matrix remained unchanged upon addition of $CaCO_3$. With increasing particle content the modulus increased and the yield strength decreased. This decrease in yield strength is due to the debonding of the particles and was similar as with rubber particles. With increasing particle content the notched impact resistance increased strongly. The notched impact energy at room temperature was increased from 10 to 80 kJ/m^2 and the brittle-to-ductile transition temperature was lowered to 80 °C. At calcium carbonate contents higher that 16 vol% no further impact improvement was observed. The calcium carbonate particles seemed to debond quite well despite the expected thermal contraction of the matrix polymer. The temperature development in the deformation zone was strong, as strong as with rubber particles. The toughening mechanism with these rigid particles is discussed.

Keywords: Calcium carbonate; Toughening; Semi-crystalline

1. Introduction

The purpose of adding mineral fillers to polymers is primarily one of cost reduction. In recent years, however, the fillers are more often used to fulfil a functional role, such as increasing the stiffness and yield strength or improve the dimension stability of the polymer [1]. However, the addition of mineral fillers generally decreases the impact energy.

A new concept is the usage of filler particles as toughening agent which at the same time increases the modulus [2–8]. The idea behind this is to mimic the rubber toughening using rigid filler particles. Like with rubber particles the rigid particles have to lower the volume strain in the matrix material so that the crazing is suppressed and shear yielding can more easily take place. For releasing the volume strain the rigid particles have to debond.

The micro-mechanism consists of three stages (Fig. 1) [3,6]:

I *Volume strain*. In a material a volume strain is generated, like ahead of a notch.
II *Debonding of the particles*. The volume strain in the matrix is released by debonding of the rigid particles.
III *Shear yielding*. In the voided matrix material the volume strain is lowered and crazing suppressed. As a result of this voiding shear yielding can take place and the material is able to absorb large quantities of energy upon fracture.

The craze mechanism becomes operative at low strains thus the debonding of the rigid particles should take place at even lower strains, prior to the yield strain. A major problem with debonding of rigid particles is the thermal contraction of the

* Corresponding author.
E-mail address: r.j.gaymans@utwente.nl (R.J. Gaymans).
[1] Present address: Artecs bv, Enschede, The Netherlands.

0032-3861/$ - see front matter © 2006 Elsevier Ltd. All rights reserved.
doi:10.1016/j.polymer.2006.05.077

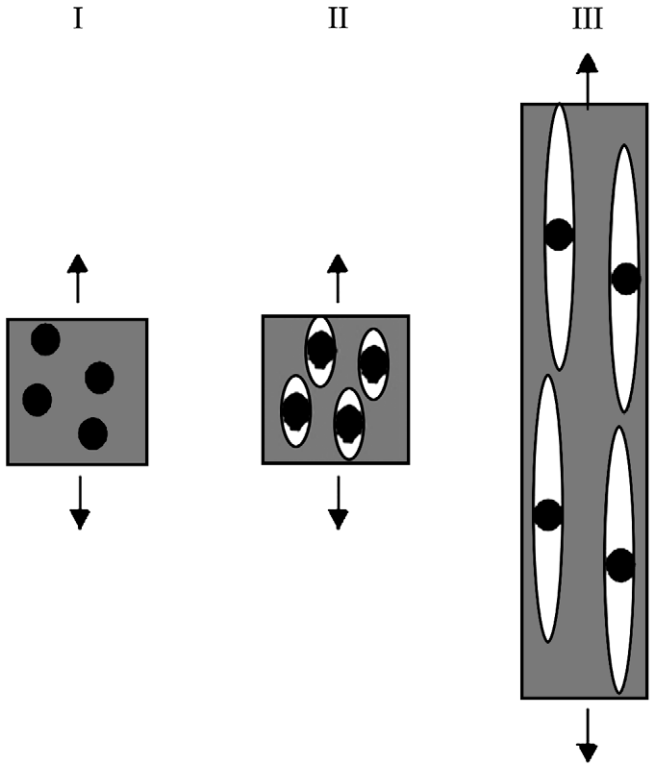

Fig. 1. Toughening mechanism with rigid particles [3,6].

matrix. The amount of thermal contraction is a function of the injection/holding pressure by injection moulding. If no pressure is applied during the cooling from the melt, the thermal contraction will be strong. As a result of debonding the yield strength is lowered and this lowering of the yield strength can be used to study the debonding of the particles [6,9]. For improved toughening the filler particles should preferably be: round (no stress concentrations); with a particle size of about 0.7 μm (large cavities are unstable); not too high interfacial tension and well dispersed [6].

The particles can also change the structure of the matrix polymer. The polymer chains at the particle surface can have a reduced mobility. In semi-crystalline copolymers this reduced mobility of polymer chains leads to the development of small and imperfect crystallites, forming a crystalline phase of low heat of fusion [10,11]. The particle can act as a nucleating agent for crystallisation and a transcrystalline layer can be formed at the particle surface [12]. The transcrystalline layer possesses higher rigidity and lower deformability, which leads to earlier crack initiation and crack propagation [13,14]. If the surface of the particle ($CaCO_3$) is coated with stearic acid the surface effects on the matrix (PP) seem to be minimal [6].

A much used filler is $CaCO_3$. The $CaCO_3$ particles are generally supplied as agglomerates and during processing these aggregates have to be broken up and dispersed into the primary particles. Large particle–particle interactions result in an incomplete breaking up of the filler agglomerates, poor appearance and inferior properties of the composites. The two major factors, which determine the particle–particle interactions, are particle size and surface free energy [4]. The analysis of adhesive forces between two bodies has demonstrated that the force acting between them depends on the curvature of the contacting surfaces and on the interaction [15,16]. Increasing amounts of aggregates in the composite lead to a drastic decrease of impact resistance of polymer-composite [6,17–19]. The most used technique to change the particle–particle and polymer–particle interactions is the coverage of filler surface with a low molecular weight organic compound [10,16,20]. For $CaCO_3$ stearic acid often is used [4,6,20]. As a result of the stearic acid coating the surface free energy of the $CaCO_3$ (210 mJ/m^2) can be reduced to 40–50 mJ/m^2 [4,20]. The stearic acid has in these systems two functions. It reduces the particle–particle interaction and this will lead to a better dispersion of the particles in the host matrix polymer. Also the polymer–particle adhesion is lowered and this eases the debonding of the particles on deformation of the composite. The stearic acid coating on $CaCO_3$ improved the dispersion in PP and increased the fracture toughness of the system [6]. With rigid particles a toughening and at the same time an increase in the modulus were found in PE [4,21–23], PP [2,5–7], PP–EPDM [24–26], and PA-6 [27]. The toughening effect of $CaCO_3$ particles on PE is good, on PP fair and on PP–EPDM and PA poor.

Aliphatic polyketone copolymers (aPK) are semi-crystalline materials with a glass transition temperature at 15 °C and a melting temperature at 225 °C [28]. These aPK have a high yield stress and high unnotched fracture toughness; however, with a notch they fracture in a brittle manner. The aPK can be toughened with rubber particles at the cost of the modulus [29]. Studies are on whether aPK can be toughened with $CaCO_3$ particles and how effective is this toughening when compared to rubber particles.

2. Experimental

2.1. Materials

Aliphatic polyketone copolymer (aPK) was kindly supplied by SHELL (Carilon P1000). The aPK is a perfect alternating copolymer, polymerised from ethylene and carbon monoxide; 6 mol% of the ethylene is replaced by propylene to lower the melting temperature (Fig. 2).

The polyketone has a glass transition temperature of approximately 15 °C and a melting temperature of 225 °C, a crystallinity of 35% and a density of 1240 kg/m^3.

Precipitated calcium carbonate was kindly given by Minerals Technologies Inc. The $CaCO_3$ is supplied with agglomerates of 0.7 mm particles coated with 1% of stearic acid, the particle size distribution was narrow ($d_w/d_n = 1.1$). The density of the $CaCO_3$ is 2710 kg/m^3.

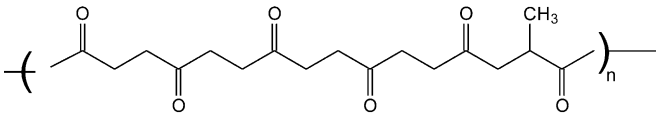

Fig. 2. Structure of aliphatic polyketone based on ethylene–ketone and propylene–ketone.

Table 1
$CaCO_3$ particle content in aPK–$CaCO_3$ composites

wt%	0	10	20	30	40	50
vol%	0	4.9	10.3	16.4	23.4	31.5

A series of composites were studied with composition varying from 0 up to 50 wt% $CaCO_3$ particles. With the given densities the volume fractions were calculated (Table 1).

2.2. Specimen preparation

Compounding of the materials was done using a Berstorff (ZE 25 × 33D) twin screw extruder. In the extrusion step, barrel temperatures were set at 225/240/240/240/240/240/240 °C and a screw speed of 140 rpm. The *L*/*D* ratio of the screws was 33 and $D = 25$ mm. During the extrusion process stabilisers for the aPK were added, 0.2 wt% Calcium-Hydroxy-Apatite (melt stabilisation), 0.3 wt% Nucrel (ethylene–methacrylic acid copolymer, processing aid) and 0.2 wt% naugard 2-2′-oxamidobis(ethyl-3(3,5 di-*t*-butyl-4-hydroxyphenyl)propionate), anti-oxidant). After compounding, the blends were injection moulded into rectangular bars (ISO 180) using an Arburg Allrounder 221-55-250 injection moulding machine. The barrel had a flat temperature profile of 240 °C, the mould temperature was kept at 70 °C with an injection pressure of 55 bar and a holding pressure of 45 bar. A single-edge V-shaped notch of 2 mm depth and tip radius 0.25 mm was milled in the moulded specimens.

2.3. SEM photography

The morphology of the compound was studied by SEM. Specimens for analysis were prepared by cutting with a Cryo-Nova microtome at −120 °C using a diamond knife (−110 °C) and cutting speed of 1 mm/s. The core of the injection moulded bars is studied. The cut surfaces were then sputter-coated with a thin gold layer and studied with Hitachi S-800 field emission SEM.

2.4. Notched Izod impact test

Notched Izod impact tests were carried out using a Zwick pendulum. To vary the test temperature, the specimens were placed in a thermostatic bath. The impact strength was calculated by dividing the absorbed energy by the initial cross-sectional area behind the notch (32 mm^2). All measurements were carried out in 10-fold.

2.5. Differential scanning calorimetry

DSC spectra were recorded on a Perkin Elmer DSC7 apparatus, equipped with a PE7700 computer and Tas-7 software. Dried sample (2–5 mg) was heated at a rate of 20 °C/min. The peak temperature of the second scan was taken as the melting temperature of the polymer; the peak area was used to determine the enthalpy.

2.6. Dynamic mechanical analysis

A Myrenne ATM3 torsion pendulum was used at a frequency of approximately 1 Hz. The storage modulus G' and the loss modulus G'' were measured. The samples ($50 \times 8.8 \times 2.2$ mm) were first cooled to −100 °C and subsequently heated to a temperature where the storage modulus G' would drop to below 15 MPa. This temperature is defined as the flow temperature (T_{flow}). During heating, 1.0 °C/min, a measurement was done every 5 °C.

2.7. Tensile tests

Tensile tests were conducted on dumbbell shaped specimens (ISO 527) with a Zwick tensile Z02 tester; all tests were carried out in fivefold. Test speed was constant at 60 mm/min (0.01 s^{-1}), standard engineering curves were obtained, the modulus was determined in the strain regime of 0.1–0.25% strain, the yield stress was taken at the first point where $d\varepsilon/d\sigma = 0$. The strain was monitored with extensometers attached to the specimen.

2.8. Infrared thermography

The temperature rise during fracture of a notched tensile specimens of thickness 4 mm was monitored using an infrared camera, the camera specifications are listed in Ref. [6]. With the infrared camera, only temperatures at the surface of the specimen can be determined. The spot size of about 100 μm is relatively large. The temperature that is indicated in one spot is an average temperature over the entire spot size.

3. Results and discussion

3.1. Introduction

The aPK–$CaCO_3$ composites are white materials and on deformation no further stress whitening is observed.

3.2. Morphology

The primary particle size of the $CaCO_3$ used was 0.7 μm, with a small particle size distribution. The particles had been treated with a stearic acid in order to obtain a better dispersion. The $CaCO_3$ particles have an aspect ratio close to unity and do not have sharp edges. The particles in the composites are quite well dispersed, but there are some small agglomerates (Fig. 3).

From the micrographs it is not clear whether the amount of agglomerates or their size change with particle content. Not clear either is whether the primary particles remain intact or that some $CaCO_3$ particles are fractured during compounding.

3.3. Thermal properties

aPK is a semi-crystalline polymer and the crystallinity might be a function of $CaCO_3$ particle content. The thermal

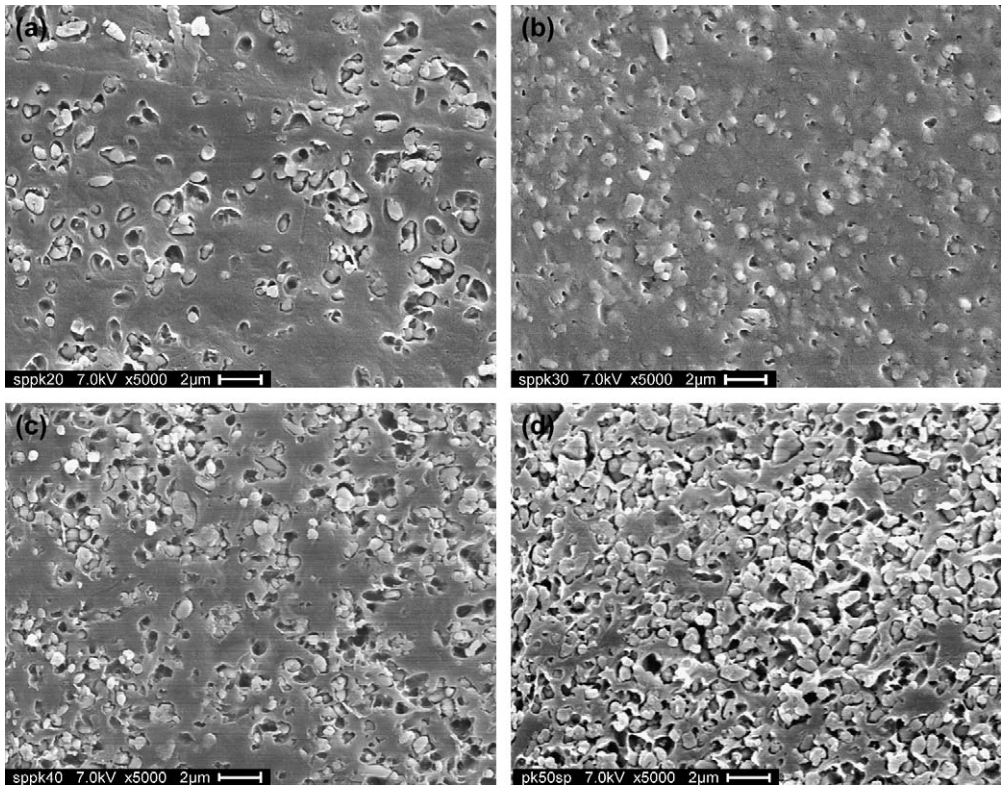

Fig. 3. Morphology of aPK–$CaCO_3$ composites with 0.7 µm coated particles, with different $CaCO_3$ contents: a, 10.3 vol%; b, 16.5 vol%; c, 23.4 vol%; d, 31.5 vol%.

properties have been determined by DSC and DMA measurements. The melting temperature of aPK is independent of particle content (Fig. 4).

The melting enthalpy (per gram polymer) decreases somewhat with particle content (Fig. 4). This lowering of the melting enthalpy suggests a lowering of the aPK crystallinity. The slightly lower crystallinity of aPK might be due to the coated $CaCO_3$ particles, however, the coated $CaCO_3$ particles had no effect on the crystallinity of PP [6].

The storage modulus and the loss modulus as function of temperature give two transitions (Fig. 5): a glass transition at 15 °C and a melting transition at 220 °C. The $CaCO_3$ content had no effect on either transition temperatures.

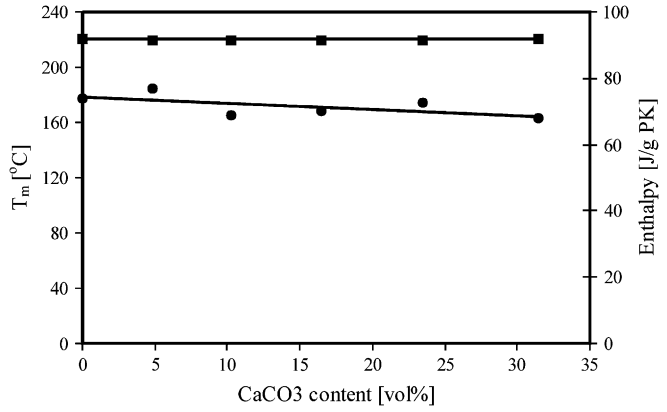

Fig. 4. Thermal properties (DSC) as a function of particle content: ■, T_m; ●, melting enthalpy.

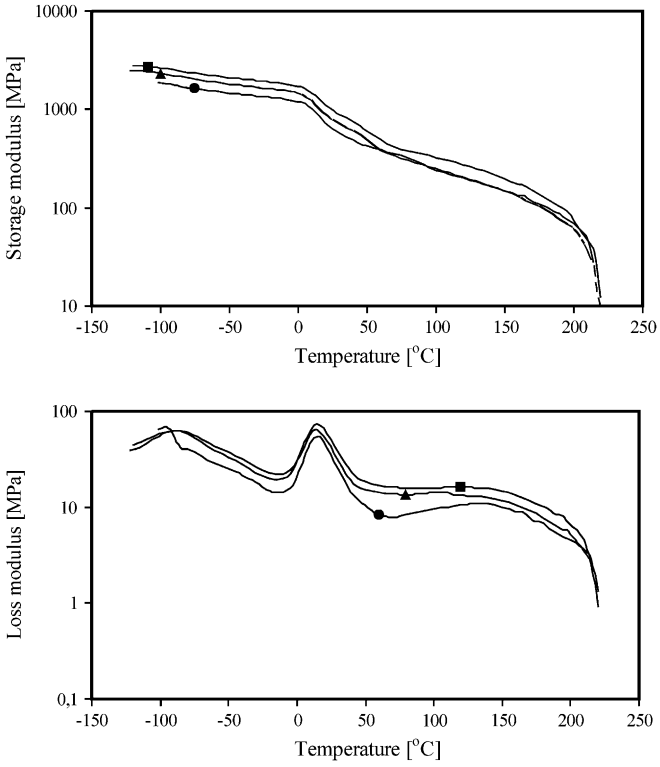

Fig. 5. Storage and loss modulus as a function of temperature for aPK–$CaCO_3$ composites with different $CaCO_3$ contents: ●, 0 vol%; ▲, 7.5 vol%; ■, 16.4 vol%.

The polymer layer near the surface of the particles might be restricted in its mobility to some extent, but it did not lead to a change in T_g of the polymer. The melting temperature with DMA corresponds to the melting temperature measured by DSC. The storage modulus is increased with filler content over the entire temperature range and the effect seems to be stronger below T_g than above T_g.

3.4. Tensile properties

Stiffness is one of the basic properties of composites and usually one of the reasons to use a filler. The modulus of composites is often modelled; the tensile modulus increases with filler content in a non-linear manner. This non-linearity is predicted by many models, such as the Einstein–Guth or Kerner or Lewis–Nielsen models [30]. In the Einstein–Guth relationship the modulus of the filler is assumed to be very high compared to the matrix modulus.

The modulus is a low strain property and in this low strain regime the adhesion between particle and polymer remains intact. Fig. 6 shows the tensile modulus of the composites plotted as a function of the $CaCO_3$ content.

The modulus of the $CaCO_3$ filled aPK increases with increasing particle content. The increase is, however, less than calculated with the Einstein–Guth relationship. Possibly the stearic acid coating is debit to this.

The yield stress is measured at much higher strains than the modulus. If the adhesion between the particle and the matrix at the yield point is still intact then the yield stress increases. However, if debonding of the particles takes place before the yield point is reached then the yield stress is lowered. The debonded particles behave as holes. The yield stress is thus sensitive for the debonding of the particles and the change in yield stress can be used to estimate the extent of debonding. In the aPK–$CaCO_3$ system the yield stresses decreased linearly with particle content (Fig. 7).

The room temperature yield stress of aPK is 70 MPa and with 16.4 vol% $CaCO_3$ particles this yield stress drops to 47 MPa which is a lowering of 33%. This decrease is not only at high temperatures (20, 60 and 100 °C) but also at

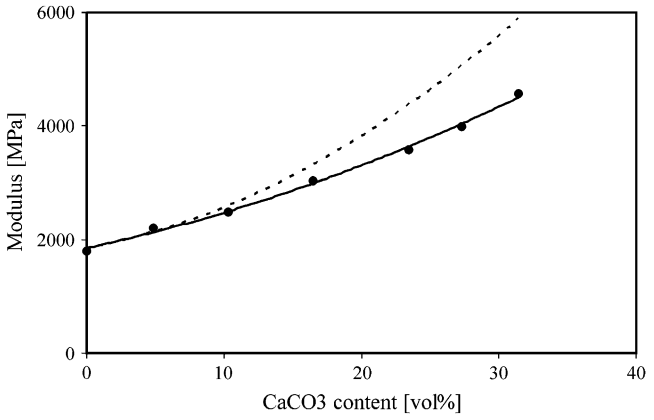

Fig. 6. Tensile modulus as a function of $CaCO_3$ content ($\varepsilon = 0.01\ s^{-1}$, $T = 23$ °C). The dashed line is calculated with the Einstein–Guth relationship [30].

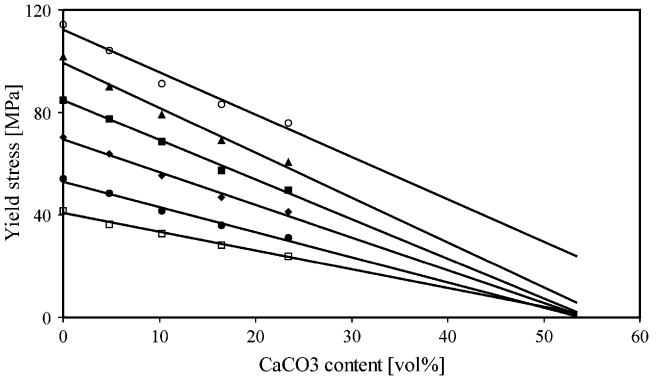

Fig. 7. Yield stress as a function of $CaCO_3$ content at different temperatures, $\varepsilon = 0.01\ s^{-1}$: ○, −40 °C; ▲, −20 °C; ■, 0 °C; ◆, 20 °C; ●, 60 °C; □, 100 °C.

low temperatures (0, −20 and −40 °C). When the yield stress decline is extrapolated to zero stress, assuming that all particles debond from the matrix polymer, a maximum fill factor is obtained (53 vol%). At very low temperatures (−20 and −40 °C), the lowering of the yield stress is somewhat less strong. This must have its origin in a smaller amount of debonding of the particles at these low temperatures. At low temperatures the effect of thermal contraction of the matrix is expected to be strongest. The results suggest that the debonding of the $CaCO_3$ particles at low temperatures is still taking place but to a lesser extent.

3.5. Impact resistance

By debonding of the particles the volume strain is (partly) relieved and thereby the stress state altered in the vicinity of the debonded particles. If the volume strain is relieved, crazing is suppressed and shear yielding can take place (Fig. 1). This mechanism is similar to that of cavitation in rubber toughened blends. Thus debonding is necessary otherwise no impact improvement can be expected in particle filled systems.

The fracture toughness of these semi-ductile materials is studied with notched Izod. The critical parameter in these materials is the transition from semi-ductile to ductile. At this transition there is considerable deformation in the notch and thus LFEM analysis under these conditions is not allowed.

The semi-ductile aPK has a fracture toughness that steadily increases with temperature and reached a ductile fracture as judged by the fracture surface at about 100 °C (Fig. 8).

By the particle filled systems the fracture toughness as function of temperature has S-shaped curves. At low temperature (0 °C) impact values seem to be independent of particle content. At higher temperatures the fracture energy increases considerably with particle content and at the same time the brittle-to-ductile transition is shifted towards lower temperatures, this at least up to a particle content of 16.4 vol%. With this 16.4 vol% $CaCO_3$ it is now possible to create ductile fracture at room temperature in the notched Izod impact test while the neat aPK shows a brittle behaviour. The fracture energy at room temperature is increased from 10 to 80 kJ/m^2 and the modulus from 1850 to 3030 MPa. This large energy

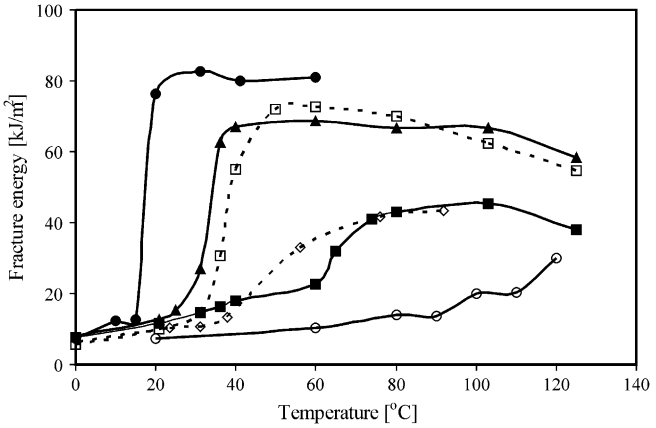

Fig. 8. Notched Izod impact energy as function of temperature, aPK–$CaCO_3$ composites as function of $CaCO_3$ content: ○, aPK; ■, 4.9 vol%; ▲, 10.3 vol%; ●, 16.4 vol%; □, 23.4 vol%; ◇, 31.5 vol%.

consumption in the composite stems mainly from the shear yielding of the aPK. The debonding of the rigid inclusions is expected not to consume large quantities of energy but is necessary to enhance the plastic deformation of the aPK.

The highest concentrations 23.4 and 31.5 vol% are surprisingly far less effective in improving the fracture toughness. The brittle–ductile transition increases again and the fracture toughness in the ductile region is lowered. The 31.5 vol% sample nearly behaves in the same manner as the 5.4 vol% sample. This poor toughening effect at high contents may be partly due to poorer debonding of the particles and/or poorer dispersions of the particles. Above 0 °C the lowering of the yield stress with particle content does not show anomalies. Agglomerate particles will lead to larger holes which are unstable and can grow into cracks, inducing more brittle behaviour [6,13,31].

An important feature of the deformation behaviour of semicrystalline polymers and their toughened blends is the brittle-to-ductile transition temperature [32]. The brittle–ductile transition temperature decreases with particle content up to 16.4 vol% and at higher contents increases again (Fig. 9).

A similar behaviour was observed with the PP–$CaCO_3$ system [6]. If the results of the $CaCO_3$ toughening of aPK are compared to the rubber toughening [28] then up to 12.5 vol% great similarities between the two systems are observed. At higher contents the rubber is more effective. With the rubber blends the T_{bd} is lowered far below the glass transition temperature of aPK [28]. Thus the glass transition of the aPK cannot be the limit for toughening. The debonding of the $CaCO_3$ particles at low temperatures (−20 and −40 °C) is somewhat less effective (Fig. 6), but it is questionable whether this is the main reason for the lower fracture toughness at high loadings.

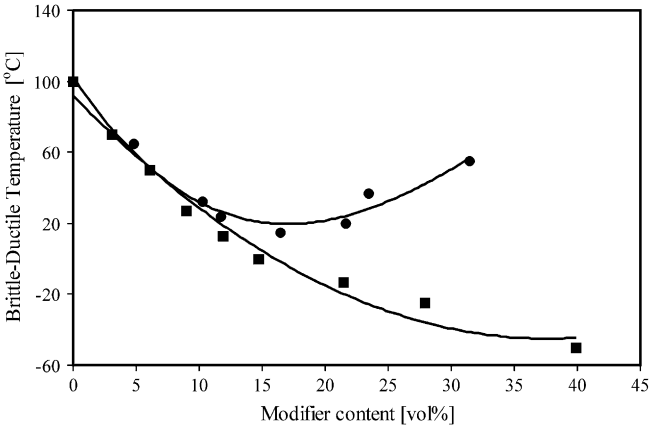

Fig. 9. Brittle–ductile transition temperature (T_{bd}) as a function of modifier content: ●, $CaCO_3$ particles; ■, rubber particles [28].

3.6. Fracture mechanism

A striking aspect of the deformation behaviour of polymer–rubber blends is the occurrence of stress whitening in deformed samples as a result of the rubber cavitation [33,34]. As aPK–$CaCO_3$ is very white, the stress whitening due to particle debonding is not visible and in this way the size and shape of the deformation zone cannot be seen. The deformation zone is studied with SEM on impacted aPK–$CaCO_3$ sample. At a large distance from the fracture surface a zone with debonded particles is visible but the voids are apparently not deformed (Fig. 10b).

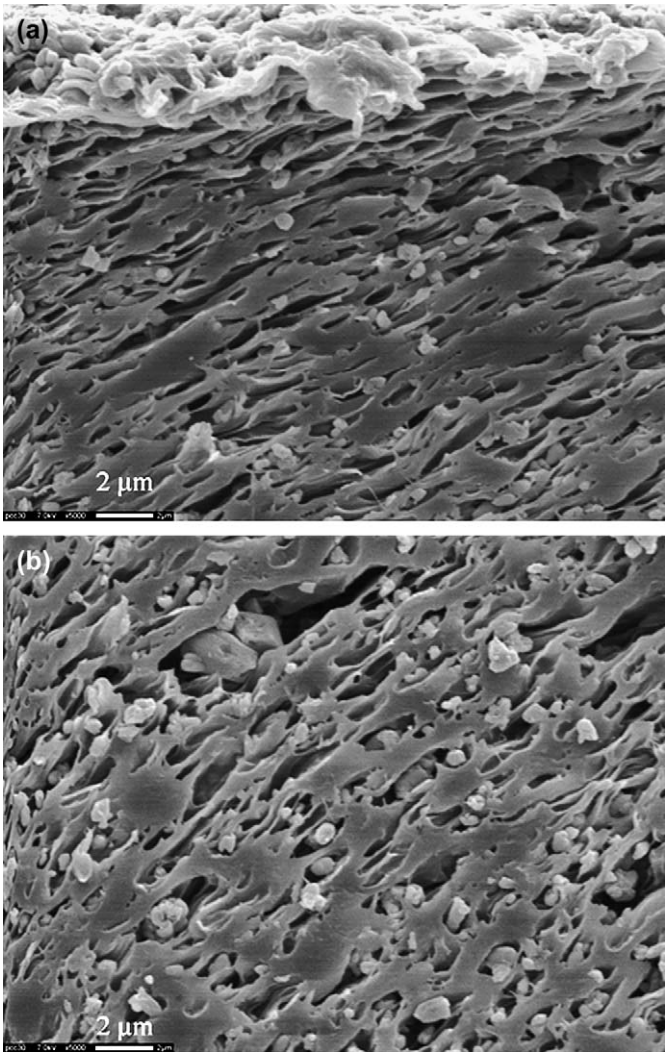

Fig. 10. Morphology below the fracture surface, 16.4 vol% $CaCO_3$ particles, after a notched Izod test.

Closer to the fracture plane the voids become strongly deformed, and have ellipsoid shapes (Fig. 10a). The crack has run from left to right. It is clear that in aPK–$CaCO_3$ the voids are present up to the fracture plane. The aPK–rubber blend has a relaxation layer next to the fracture surface [29]. Such a relaxed layer was not observed in these aPK–$CaCO_3$ composites. The aspect ratio of the voids is a measure for the deformation strain of the matrix polymer next to the voids. At the fracture plane the voids are strongly elongated and the strains of the thin ligaments seem to be well above the natural draw ratio of the aPK (300–350%). The voids of the 0.7 μm debonded particles are stable in the sense that they do not seem to have coalescence with each other to larger voids. This is an important feature of the fracture mechanism; if the cavities grow to a very large size they could initiate early fracture of the material. With increasing distance from the fracture plane the deformation of the voids is lowered and thus the deformation in the matrix is lowered.

3.7. Infrared thermography

It is known that when polymers are subjected to high strain rates, the deformation process becomes adiabatic. As a result of this the temperature in the deformation zone rises and this has large consequences for the fracture process. At increasing temperatures the yield stress is lowered and more deformation is possible, which again increases the temperature. This is a self-reinforcing process and the temperature can eventually rise up to the melting temperature of the polymer [29]. At high temperatures ahead of a notch and/or crack yield stress is low and considerable deformation can take place. Due to this large deformation the notch is blunted (thermal blunting) and the stress concentration lowered. To monitor the temperature development during fracture an infrared camera was used. Experiments have been conducted on notched samples at an apparent strain rate of 0.03 s^{-1} (Fig. 11). The spot size of the camera was 100 μm, which is quite large compared to the thickness of the deformation zone.

The temperature rise is indicative of the amount of plastic deformation. On increasing sample strain the ''dark'' deformation zone ($\Delta T \sim 3$ °C) develops from a small spherical zone towards a zone with two lobes developing under a 45 degree angle. The width of this zone increases. Ahead of the notch there is a strong temperature development ($\Delta T > 60$ °C) and the notch is clearly blunted. The zone size of the strongly warmed material ahead of the running crack (last picture) increases to about 300 μm.

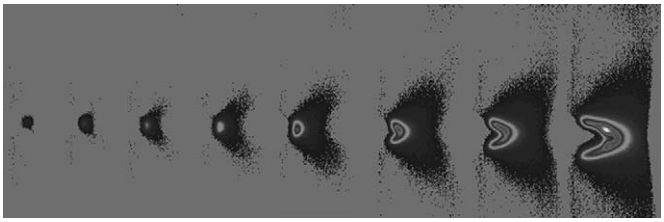

Fig. 11. Development of process zone (in eight steps) of a notched sample (20.3 vol% $CaCO_3$) during fracture, at an apparent strain rate 0.03 s^{-1}, by infrared thermography. The threshold value for the background was 21 °C.

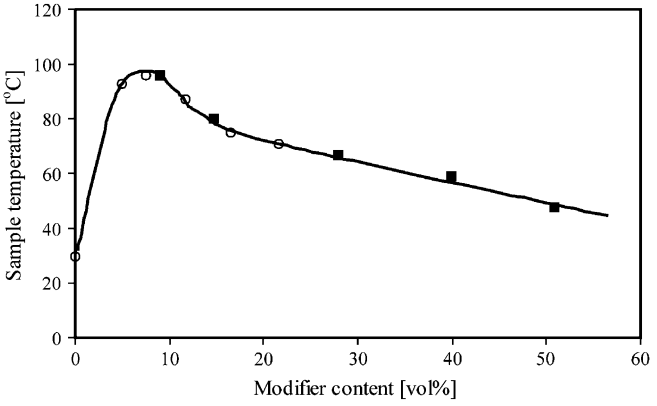

Fig. 12. Maximum sample temperature during fracture of aPK–$CaCO_3$ composites and aPK–rubber blends at 0.03 s^{-1} [29]: ○, aPK–$CaCO_3$; ■, aPK–rubber.

aPK fractures in a brittle fashion, has a small plastic zone size and small temperature increase. Upon addition of a small amount of filler particles the temperature rises from 30 °C up to 95 °C (Fig. 12).

At higher strain rates this temperature effect is expected to be stronger. With aPK the temperature increases to 24 °C per decade strain rate [35]. The strain rate at impact is about a three decades higher and thus about a 72 °C higher than the temperatures in Fig. 12.

With increasing particle content the maximum temperature is lowered. At the same time the size of the plastic zone is increased considerably. The lower maximum temperatures at increasing contents can be due to the lower amount of polymer that is deformed and/or the wider deformation zone that lowers the strain rate. The temperature development of the aPK–$CaCO_3$ composites with concentration shows the same trend as was found for aPK–rubber blends [29]. The $CaCO_3$ particles fulfil the same function as a toughener as the rubber particles.

4. Conclusions

It has been shown that the addition of the $CaCO_3$ particles, 0.7 μm in size and coated with stearic acid, increases the notched impact energy at room temperature from 10 to 80 kJ/m^2 and lowers the brittle-to-ductile transition temperature (T_{bd}) by 80 °C. At the same time the modulus increased but the yield stress was lowered. The lowering of the yield stress is due to the debonding of the calcium carbonate particles prior to the yield stress. The main deformation step in the toughening process with these particles is the debonding of the particles. The toughening effect of these particles is as effective as with rubber particles. This suggests that after debonding of particles, the particles have no effect on the impact behaviour. Also the thermal properties of the matrix polymer are little affected by the addition of $CaCO_3$ particles.

At $CaCO_3$ contents higher than 16 vol% the impact properties were not further improved. The debonding of the particles at high loadings as judged by the lowering of the yield stress, was still taking place, even at very low temperature (−40 °C); however, at very low temperatures somewhat less effective. The reason for this relatively poor impact behaviour at high $CaCO_3$ contents might partly be due to a poorer delamination at low temperatures.

Acknowledgments

This research was financed by Shell Research and Technology Centre Amsterdam. The authors would like to thank Mr. P.J. Fennis and Dr. A.A. Smaardijk for their contribution and helpful discussions.

References

[1] Baker RA, Koller LL, Kummer PE. Handbook of fillers for plastics. 2nd ed. NY: Van Nostrand Reinhold; 1987.
[2] Pukánszky B. Polypropylene: structure, blends and composites. In: Karger-Kocsis J, editor. London: Chapman and Hall; 1995 [chapter 1].
[3] Kim GM, Michler GH. Polymer 1998;39:5689.
[4] Bartczak Z, Argon AS, Cohen RE, Weinberg M. Polymer 1999; 40:2347.
[5] Thio YS, Argon AS, Cohen RE, Weinberg M. Polymer 2002;43:3661.
[6] Zuiderduin WCJ, Westzaan C, Huétink J, Gaymans RJ. Polymer 2003;44:261.
[7] Wang K, Wu JS, Ye L, Zeng H. Composites Part A 2003;34(11):1199–205.
[8] Dubnikova IL, Berezina SM, Oshmyan VG, Kuleznev VN. Polymer Science Series A 2003;45:873.
[9] Pukánszky B. Composites 1993;21:255.
[10] Kowaleski T, Galeski A. Journal of Applied Polymer Science 1986;32:2919.
[11] Maurer FHJ, Schoffeleers HM, Kosfeld R, Uhlenbroich T. Progress in science and engineering of composites. Tokyo: ICCM-IV; 1982. p. 803.
[12] Burton RH, Day TM, Folkes MJ. Polymer Communications 1984; 25:361.
[13] Riley AM, Paynter CD, McGenity PM, Adams JM. Plastic and Rubber Processing and Applications 1990;14:85.
[14] Folkes MJ, Hardwick SJ. Journal of Materials Science Letters 1987;6:656.
[15] Tabor D. Journal of Colloid and Interface Science 1977;58:2.
[16] Roberts AD. Rubber Chemistry and Technology 1979;52:23.
[17] Bucknall CB. Performance. In: Paul DR, Bucknall CB, editors. Polymer blends, vol. 2. NY: John Wiley & Sons, Inc; 2000 [chapter 22].
[18] Varga J. Journal of Thermal Analysis 1989;35:1891.
[19] Svehlova V, Poloucek E. Angewandte Makromolukulare Chemie 1987;153:197.
[20] Suetsugu Y, White JL. Advances in Polymer Technology 1987;7:427.
[21] Wang Y, Lu J, Wang GJ. Journal of Applied Polymer Science 1997;64:1275.
[22] Hoffmann H, Grellmann W, Zilvar V. Polymer composites. NY: Walter de Gruyter; 1986.
[23] Badran BM, Galeski A, Kryszewski M. Journal of Applied Polymer Science 1982;27:3669.
[24] Ling Z, Li CZ, Rui H. Journal of Polymer Science Part B 2005; 43:1113.
[25] Chen JF, Wang GQ, Zeng XF, Zhao HY, Cao DP, Yun J, Tan CK. Journal of Applied Polymer Science 2004;94:796.
[26] Zhang L, Li CZ, Huang R. Journal of Polymer Science Part B 2004; 42:1656.
[27] Plummer CJG, Mauger M, Béguelin P, Orange G, Varlet J. Polymer 2004;45:1147.
[28] Zuiderduin WCJ, Homminga DS, Huétink J, Gaymans RJ. Polymer 2004;44:6361.
[29] Zuiderduin WCJ, Vlasveld DPN, Huétink J, Gaymans RJ. Polymer 2004;45:3765.
[30] Nielsen LE. Mechanical properties of polymers and composites. NY: Marcel Dekker; 1974.
[31] Pukansky B, Tüdös F, Kolarik J, Lednický F. Polymer Composites 1990;11:98.
[32] Vollenberg PHT, Heikes D. Polymer 1989;30:1656.
[33] Ramsteiner F, Heckmann W. Polymer Communication 1985;26:199.
[34] Gaymans RJ. Performance. In: Paul DR, Bucknall CB, editors. Polymer blends, vol. 2. NY: John Wiley & Sons, Inc; 2000. p. 177 [chapter 25].
[35] Zuiderduin WCJ. Deformation and fracture of aliphatic polyketones. Thesis, University of Twente: 2002 [chapter 3].